applied sciences

MDPI

Article

Implementation of Shape Memory Alloy Sponge as Energy Dissipating Material on Pounding Tuned Mass Damper: An Experimental Investigation

Jie Tan [1,2], Jinwei Jiang [3,*], Min Liu [4], Qian Feng [1,2], Peng Zhang [5] and Siu Chun Michael Ho [3,*]

1 Hubei Key Laboratory of Earthquake Early Warning, Institute of Seismology, China Earthquake Administration, Wuhan 430071, China; tanjie@hust.edu.cn (J.T.); qfengwh@foxmail.com (Q.F.)
2 Wuhan Institute of Earthquake Engineering Co., Ltd., Wuhan 430071, China
3 Department of Mechanical Engineering, University of Houston, 4800 Calhoun, Houston, TX 77024, USA
4 School of Civil Engineering, Harbin Institute of Technology, Harbin 150090, China; liumin@hit.edu.cn
5 Institute of Road and Bridge Engineering, Dalian Maritime University, Dalian 116023, China; peng.zhang47@dlmu.edu.cn
* Correspondence: jjiang7@uh.edu (J.J.); smho@uh.edu (S.C.M.H.); Tel.: +1-713-743-4498 (J.J.); +1-713-743-4498 (S.C.M.H.)

Received: 29 January 2019; Accepted: 10 March 2019; Published: 14 March 2019

Abstract: Piping systems are important nonstructural components of most types of buildings. Damage to piping systems can lead to significant economic losses, casualties, and interruption of function. A survey of earthquake disaster sites shows that suspended piping systems are flexible and thus prone to large deformation, which can lead to serious damage of the piping systems. The single-sided pounding tuned mass damper (PTMD), which is an emerging vibration suppression tool, has the potential to serve as a cost effective and non-invasive solution for the mitigation of vibration in suspended piping systems. The operating frequency of the single-sided PTMD can be tuned similarly to a tuned mass damper (TMD). The single-side PTMD also possesses high energy dissipation characteristics and has demonstrated outstanding performance in vibration control. One of the key factors affecting the performance of the PTMD is the damping material, and there is a constant search for the ideal type of material that can increase the performance of the PTMD. This paper explores the use of shape memory alloy (SMA) sponge as the damping material for two types (spring steel and pendulum types) of PTMDs to mitigate the vibration of a suspended piping system. The PTMDs are tested both in free vibration and in forced vibration. The results are compared with no control, with a TMD control, and with a viscoelastic (VE) material PTMD control. The results show that in free vibration tests, SMA–PTMDs attenuate the displacement of the piping system significantly. The time to mitigate vibration (i.e., reduce 90% of the vibration amplitude) is reduced to 6% (for spring steel type) and 11% (for pendulum type) of the time taken to mitigate vibration without control. In forced vibration tests, the overall magnitudes of the frequency response are also lowered to 38% (spring steel) and 44% (pendulum) compared to vibration without control. The results indicate that SMA has the potential to be a promising energy dissipating material for PTMDs.

Keywords: vibration control; pounding tuned mass damper; PTMD; viscoelastic material; shape memory alloy; SMA; suspended piping system

1. Introduction

Piping systems are crucial to the functionality of commercial and industrial buildings including offices, shopping malls, hospitals, airports, and plants. The building piping systems consist of water/gas pipes, ventilation, and cable conduits, which are mounted on overhead slabs. However,

considering the significance to the operation of the building, the seismic safety of piping systems has not received the attention it deserves. As a nonstructural component, piping systems are usually based on empirical design and thus their design does not take potentially large deformations (e.g., which may occur during an earthquake) into account. To date, there is no specific seismic design code for bearing capacity including piping dynamic deformation. Thus, seismic safety of piping systems is a noteworthy issue.

The historical earthquake disaster loss survey shows that the consequences of piping system damages are multifaceted [1,2]. First, piping systems are important nonstructural components in buildings, and consist of a considerable proportion of the total building investment [3,4]. Damage to piping systems can therefore potentially result in drastic economic consequences. Second, the destruction of a piping system can cause serious secondary disasters including flooding. Both in the Hawaii earthquake (2006) [5] and the Chile earthquake (2010) [6], severe water damage occurred subsequently to piping system damage. Furthermore, the destruction of the piping system can cause the failure of function, which is unacceptable for key infrastructures including hospitals, airports, water supply companies, and fire extinguisher systems. The 1994 Northridge earthquake was a convincing example. After the earthquake, hundreds of patients had to be evacuated due to the disrupted functionality of 13 hospitals [7]. More than 100 fires were ignited and were not extinguished in time due to the destruction of fire protection systems [8]. In the San Fernando Valley, 80,000 to 100,000 people were out of water for five days due to over 3000 leaks in the water supply piping system [9].

The disaster loss investigation reports indicate that suspended piping systems with high flexibility have the most serious seismic damage [7]. In practical engineering, there are two types of suspended piping systems: one is suspended by single rods at intervals (as shown in Figure 1a), the other one is supported by trapeze hangers (as shown in Figure 1b). Both types of piping system possess high mechanical flexibility, which can lead to large deformation (i.e., strain) due to seismic loadings. The direct consequence of large deformation is structural damage caused by the collision of the piping system with adjacent components or equipment [10]. In addition, differential deformation and stress concentration are other damage types that can occur in the piping system [10]. Thus, reducing the seismic responses of the piping system can greatly improve the safety of the entire building system.

(**a**) (**b**)

Figure 1. Two types of suspended piping systems: (**a**) A single rod piping system; (**b**) trapeze hangers supporting a suspended piping system.

In new buildings, seismic braces are added to limit the deformation of the piping system. The seismic braces secure the piping system at the price of having the piping systems possibly enduring large internal forces [11,12]. However, for existing buildings, the overhead space can be filled with various equipment and facilities, which can complicate the installation of seismic braces within the limited space. Compared to seismic braces, passive dampers have the distinct advantage of reducing the vibration motions of piping system to an acceptable range. Passive dampers are widely used in the vibration control of industrial piping systems in a variety of complex environments.

In the Arctic Circle, tuned mass dampers (TMDs) were applied to mitigate wind-induced vibration of approximately 30,000 spans of pipelines. The displacement reduction factor offered by the TMD ranged from 1.5 to 7 depending on the wind conditions [13]. Due to their cost effectiveness and minimal need for maintenance, metal dampers of various shapes (X-shape, V-shape) are used as supports for nuclear plant piping systems to reduce their seismic-induced displacements [14,15]. Friction dampers are another substitute for piping system supports [16–18]. In the study by Suzuki et al. [17], with steel-steel friction supports, the displacement of the pipe was reduced by 90% under both broad-band and narrow-band excitations, and the acceleration was reduced by 50% and 80% respectively. However, these damper systems are mostly used in industrial infrastructure, and are rarely used for building piping systems (e.g., commercial and residential).

In the field of civil engineering vibration control, passive control [19–22], semi-active control [23–25], active control [26–28], and hybrid control [29–32] have been extensively studied and demonstrated. In particular, passive control is the most widely used type of control system due to its simple structure, easy maintenance and high reliability [33–35]. The pounding tuned mass damper (PTMD) is a new type of passive damper. In order to dissipate energy, the PTMD utilizes the pounding of a mass against an energy dissipating material. The natural frequency of the PTMD can be tuned to that of the host structure in order to more efficiently dissipate energy [36]. Some of the notable advantages of the PTMD are the simplicity of the design and the robustness of the device. The simplicity of the design allows the PTMD to be easily adapted to different conditions and usages; and since the PTMD is robust and can maintain its performance for long periods of time, the need for maintenance is reduced. In recent years, PTMD has been extensively studied for implementation in different types of facilities [37–40], including frame structures [41], subsea jumpers [42,43], power transmission towers [44], etc. In a previous study by the authors [45], two types of PTMDs (spring steel type and pendulum type) associated with viscoelastic (VE) material were designed. The results indicated that VE–PTMDs performed well in suppressing the vibration of a suspended piping system. With their hysteretic behavior [46], shape memory alloys (SMAs) are another popular energy dissipating material used in control systems [47–51]. As will be further discussed in the following sections, SMAs have unique material properties originating from their transition from martensite to austenite states. The phase change is highly hysteretic and is a source of energy damping, leading to the unique superelasticity and shape memory effect of SMAs. This phase change can be manipulated by controlling the temperature of the SMA [52–56], such as through an electrical current [57]. Many researchers have taken advantage of this unique property to develop adaptive TMDs in active and semi-active control schemes to enhance the damping capabilities of the TMDs [58–61]. However, SMAs have been never used in a PTMD before. Based on the demonstrated damping characteristics of SMAs, the PTMD may benefit in terms of increased performance from the integration of SMAs into its design.

In this paper, two types of PTMDs are employed to suppress the vibration of suspended piping systems. Unlike the previous experiments [45], the energy dissipating material is changed from VE material to shape memory alloy (SMA). The SMA–PTMDs are tested in free vibration and forced vibration, and the control performances are compared with a TMD control and a VE–PTMD control. The results show that SMA achieves a desirable equivalent damping coefficient to effectively suppress the vibration of the suspended piping system.

2. Pounding Tuned Mass Damper (PTMD) and Energy Dissipating Material

The earliest PTMD was proposed by Song et al. [36], on the basis of the TMD device, which consisted of a secondary mass and a swing arm and two delimiters covered with viscoelastic materials. Figure 2a shows the schematic of the double-sided PTMD. The double-sided PTMD has two vibration control mechanisms: when the excitation is small, the tuned mass will vibrate within the two delimiters as a traditional TMD; when the excitation exceeds a certain level, the tuned mass will collide with the viscoelastic material on the surface of the delimiter, dissipating the kinetic energy of the system. These

two vibration control mechanisms can enhance the vibration control effectiveness and robustness of the damper [38,42,43].

In 2017, Wang et al. [37] innovatively proposed the single-sided PTMD, which contained only one delimiter, as shown in Figure 2b. When the secondary mass was in the initial equilibrium state, it was in contact with the delimiter. Thus, the mass could only move in one direction relative to the delimiter. Due to the collision of the mass with the delimiter, the corresponding frequency of the system would become twice the original frequency, as shown in Equation (1),

$$f_{PTMD} = 2f_{TMD} = \frac{\sqrt{k/m}}{\pi} \quad (1)$$

where f_{PTMD} and f_{TMD} are the frequencies of the single-sided PTMD and conventional TMD, respectively, and k and m are the stiffness and mass of the damper. A notable advantage of the single-sided PTMD is that the gap between the mass and the delimiter is no longer a design parameter and the collision occurs at a position that could dissipate the maximum kinetic energy. The effectiveness of single-sided PTMD has been demonstrated by theoretical analysis and experimental studies [37,62].

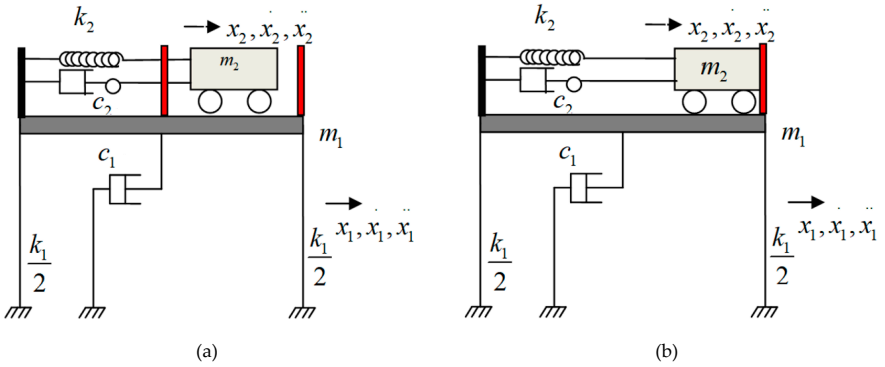

Figure 2. Schematic of (**a**) double-sided pounding tuned mass damper (PTMD); (**b**) single-sided PTMD.

Due to the simultaneous viscous and elastic characteristics, VE materials are popular in vibration mitigation and energy dissipation [63–65]. Both in the PTMD studies of Song [36] and Wang [37], VE materials were used as energy dissipating material. The performance in previous experiments proves that VE materials are suitable as an energy dissipating material for PTMD [45,66,67].

Shape memory alloys (SMAs) were discovered relatively recently [68–70], and uniquely possess both a shape memory effect (SME) and superelasticity, both of which give SMAs a highly hysteretic stress–strain relationship [71,72]. The significant hysteresis in the stress–strain relationship of SMAs makes them an ideal candidate for implementation in passive vibration control [73–76]. Applications include control of stay cables [77,78], isolation bearings [79–84], and frame braces [85,86]. Due to its high damping capacity, SMA is an ideal energy dissipating material in passive control. In theory, it is feasible to use SMA as pounding energy dissipating material for PTMD.

In this paper, the SMA is chosen as energy dissipating material for single-sided PTMD to improve its vibration control performance. To better understand the effectiveness of SMAs in energy dissipation, the vibration control effects of single-sided SMA–PTMDs are studied, and the results are compared with TMD and VE–PTMDs tested in a previous study conducted by the authors [45]. The PTMDs are employed to suppress the same suspended piping system under the same excitation conditions. In order to improve the readability and continuity of the article, the piping system and the experimental setup are presented again in this paper.

3. Modal Analysis of a Suspended Piping System

A galvanized water pipe is used as the experimental suspended piping system for testing the performance of PTMDs. The pipe with two fixtures is connected by two vertical steel bars to an

aluminum beam (1220 mm, 80 mm, 40 mm), as shown in Figure 3a. The length of the steel pipe is 1133 mm; the outer and inner diameters are 115 mm and 110.8 mm, respectively. The steel bars used to suspend the pipe are 195 mm in length and 6.35 mm in diameter. The total mass of the pipe, bars, and fixtures is 9.3 kg.

By applying a small impact load to the pipe, it can be found that the fundamental vibration mode is in the lateral direction. To determine the dynamic characteristics of the piping system, a finite element (FE) model is developed in the ABAQUS interface (Dassault Systems, Velizy-Villacoublay, France) [87]. The results of the FE analysis show that the first and the second mode shapes of the piping system consist of lateral and longitudinal motions, respectively. The mode shapes are shown in Figure 3b,c and the corresponding frequencies are 2.54 Hz and 8.14 Hz, respectively. The lower frequency lateral motion also experiences the larger displacement. Therefore, the lateral movement of the piping system is selected as the target motion for experimental studies.

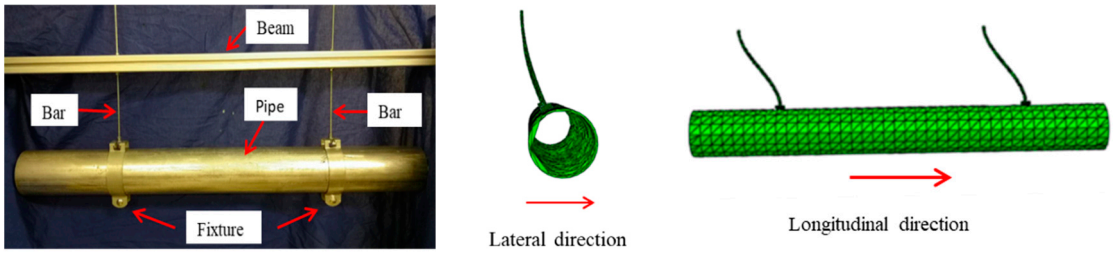

Figure 3. Piping system model and its finite element model: (**a**) Suspended piping system; (**b**) first vibration mode shape; (**c**) second vibration mode shape.

To verify the results of the FE model and also estimate the piping system viscous damping, a damped free vibration test is conducted. An initial displacement is applied to the middle of the pipe, and the displacement response of the pipe is recorded. With the help of the fast Fourier transform (FFT), the primary frequency of the piping system is 2.55 Hz, which is slightly different from the FE result (2.54 Hz). The slight difference between the obtained frequencies may be due to minor, unavoidable differences between the real and simulated model. The closeness of the obtained frequencies, on the other hand, demonstrates the accuracy of the FE analysis. Through the logarithmic decrement method, the damping ratio of the piping system is estimated to be 0.58%.

4. Experimental Setup

In the previous study by the authors [45], the TMD and VE–PTMDs were tested for the vibration control of the same piping system. For comparison, in this experiment, the mass and the swing arms of PTMD are identical to the previous study [45], except that the VE material is replaced by an SMA sponge. Figure 4 shows these two different energy dissipating materials. The shape memory alloy wire is manipulated into a cuboid shaped sponge and used as an energy dissipating layer. Its dimensions are 48 mm, 20 mm, and 10 mm, respectively. The mass used in the TMD and PTMDs is a 0.403 kg cylindrical steel block, and the corresponding mass ratio is 4.33%. The mass ratio is a key parameter of TMD, and is often designed to be in the range of 1~5%. To determine an appropriate mass ratio for TMD, the feasibility of the actual engineering application and the required vibration control effect should be taken into consideration.

To achieve the pounding between the mass of the PTMD system and the pipe, a fixture tightly sleeved around the pipe is precisely machined, and the PTMD is mounted on the fixture, which is installed at the middle of the pipe, as shown in Figure 5a. Spring steel type and pendulum type are both tested, as shown in Figure 5b,c. In single-sided PTMD, the collision occurs at the equilibrium position and the frequency is doubled after the collision [37]. Thus, the frequency of the swing arm–mass system of the PTMD should be half of the piping system's frequency (2.55 Hz), which is 1.28 Hz. When

pounding occurs, the swing arm–mass system will vibrate at 2.55 Hz and will thus be tuned to the frequency of the piping system. The natural frequency of the swing arm–mass system is tuned to 1.28 Hz through trial and error adjustments to the length of the swing arm. Results show that the target frequency is achieved when the length of the spring steel and the length of the nylon rope are 170 mm and 128 mm, respectively. The detailed parameters of the PTMDs are listed in Table 1.

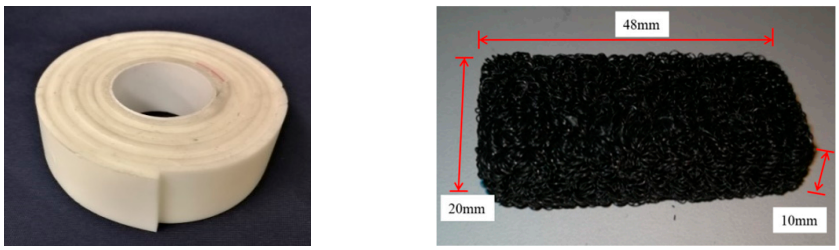

(**a**) (**b**)

Figure 4. Energy dissipating materials used in PTMD: (**a**) Viscoelastic (VE) material; (**b**) shape memory alloy (SMA) material in the form of sponge.

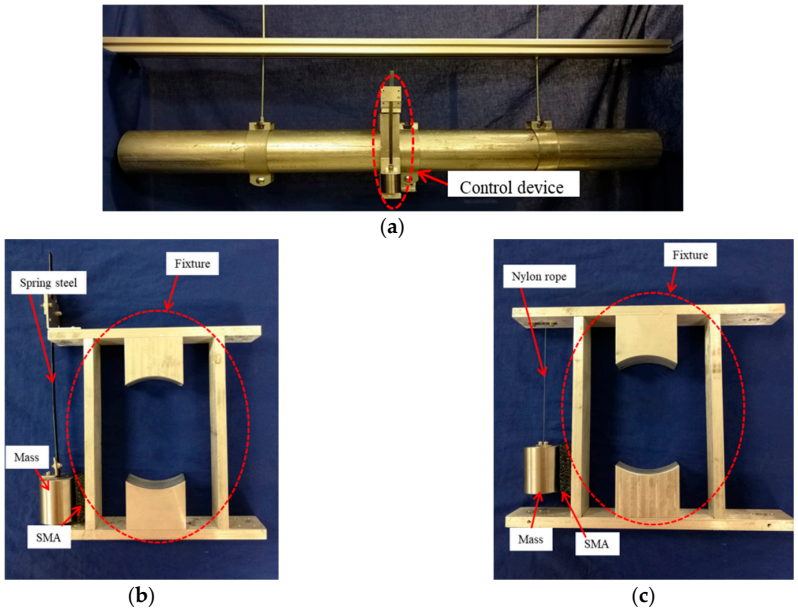

(**a**)

(**b**) (**c**)

Figure 5. (**a**) Control device installed at the piping system; (**b**) spring steel type SMA–PTMD; (**c**) pendulum type SMA–PTMD.

Table 1. Parameters of PTMDs (pounding tuned mass dampers).

PTMD (Spring steel type)	Frequency of the spring steel–mass system	1.28 Hz
	Component / Description	Value
	Spring steel / Material	Spring steel
	Spring steel / Dimensions (mm)	170 × 6.5 × 0.4
PTMD (Pendulum type)	Frequency of the pendulum–mass system	1.28 Hz
	Component / Description	Value
	Nylon rope / Material	Nylon
	Nylon rope / Length (mm)	128
Mass for PTMDs	Material	Steel
	Weight (kg)	0.403
Energy dissipating material	SMA	48 × 20 × 10 (mm)

During the experiment, a laser displacement sensor (MX1A-A, IDEC Sensors, Tokyo, Japan) with a range of ±40 mm is installed at a separate table not coupled to the piping system to record the

displacement response of the piping system. The sampling frequency of the laser sensor is set to 200 Hz. In the forced vibration experiment, a high-power DC motor (DC-158A, AVIC, Beijing, China) with a rotating arm is used as the excitation source. A bungee cable is used to connect the pipe and the rotating arm. In order to ensure excitation in the horizontal direction only, a pulley is installed to turn the bungee cable by 90 degrees. A wide range of excitation frequencies can be achieved by changing the motor's angular speed. Figure 6a,b show the experimental setup of the forced excitation system and the data acquisition system, respectively. The power supply (CSI3020SW, CircuitSpecialists, Tempe, AZ, USA) is used to change the rotating speed of the motor, and the data is collected by the laser sensor through a laptop and a data acquisition card (NI USB X Series 6361, National Instruments, Austin, TX, USA).

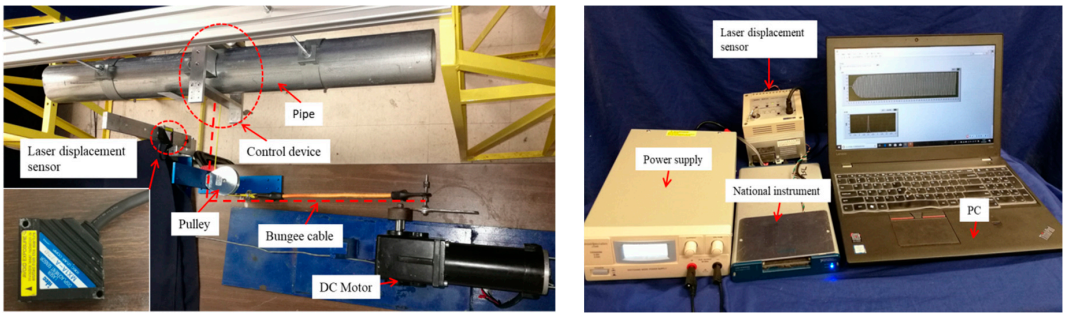

(**a**) (**b**)

Figure 6. (**a**) Experimental setup and (**b**) data acquisition system.

5. Results and Discussion

In this section, two types (spring steel type and pendulum type) of SMA–PTMDs are employed to suppress the vibration motions of the suspended piping system both in free vibration and in forced vibration. In the previous study [45], the performances of TMD and VE–PTMDs on suppressing the vibration of the piping were experimentally compared. In this paper, the effectiveness of SMA–PTMDs is verified by the comparative results of the piping system without a control, with a TMD control, and with a VE–PTMD control.

It is notable that the mass and the swing arm (spring steel) of the TMD are the same as that of the spring steel type PTMDs. The damping of the TMD is very small (0.06%) due to the lack of auxiliary damping and the low damping capacity of the spring steel. The TMD is not optimally designed for two reasons. First, the TMD and PTMDs (spring steel type) have the same configurations except that in the PTMDs, the mass collides with the energy dissipating material. Both the TMD and PTMDs are tested to suppress the vibration of the same suspended piping system. By this approach, the effect of the pounding on the resulting damping can be compared directly. Secondly, achieving a specific amount of damping for TMDs (i.e., the optimum damping) is challenging. The desired level of damping in the PTMD is accomplished by adjusting the level of pounding between the mass and the energy dissipating material and is free of maintenance. In this aspect, the TMD and PTMDs are kept at the same complexity to compare their vibration mitigation performance.

5.1. Suppression of Free Vibration

During free vibration tests, an initial displacement is applied to the piping system, and the displacement response is recorded. Figure 7 illustrates the time domain displacement curves of the piping system under the control of TMD and PTMDs. For a clear comparison, the initial displacement of the free vibration is 20 mm for all conditions and the time from the initial displacement to decay to 10% of the initial displacement (2 mm) is defined as the control time. Figure 7a illustrates the displacement response of the piping system subject to free vibration with and without TMD control. The control times are 26.5 s (without control) and 48.8 s (with TMD control), and the corresponding damping ratios are 0.58% and 0.29%, respectively. As shown in Figure 7b,c, when VE–PTMDs are

employed, the vibration attenuation is more pronounced. The control times are 1.6 s (with spring steel type VE–PTMD) and 2.85 s (with pendulum type VE–PTMD), respectively, and the corresponding system damping ratios are 10.4% and 5.6%.

Figure 7d,e show the free vibration responses of the piping system with spring steel type SMA–PTMD control and with pendulum type SMA–PTMD control, respectively. The beating phenomenon is observed for both types of SMA–PTMDs, and is different from the smoothly decaying trend of vibration intensity with VE–PTMDs control. The responses of the SMA–PTMDs are similar, and only one beat cycle is observed. First, the displacements decay rapidly to zero, then slightly increase, and then decrease gradually. From visual observation, when an instantaneous displacement is applied to the piping system, the SMA–PTMD worked immediately with strong poundings. When the displacement decayed rapidly to zero, the displacement of the mass of the PTMD is observed to be large. The beating suggests the transferal of energy between the piping system and the mass of the PTMD. Following the approach to zero displacement, the impact of the mass onto the pipe induces a small increase in the displacement. Finally, successive collisions between the mass of the PTMD and the pipe attenuate the displacement of the pipe to zero.

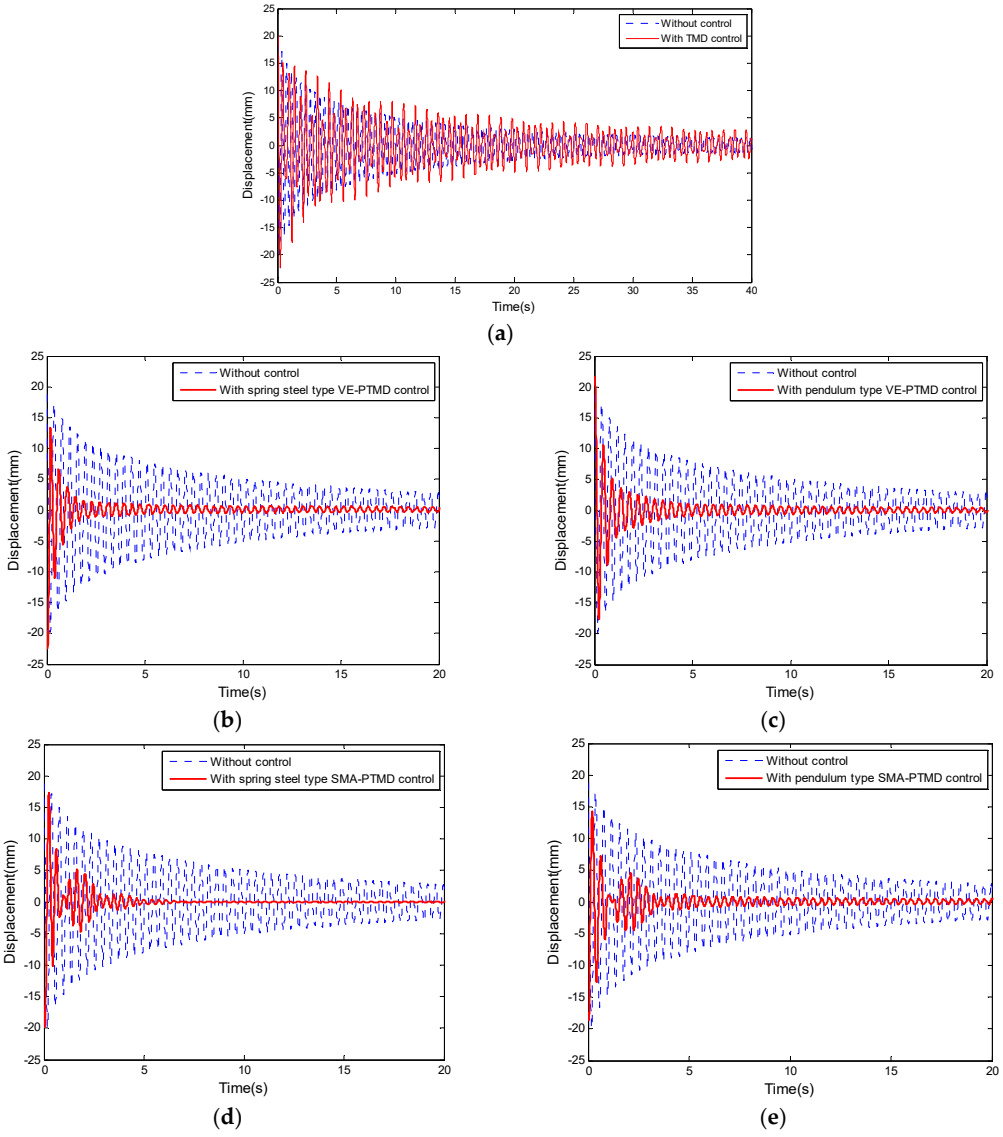

Figure 7. Experimental results of free vibration: (**a**) With tuned mass dampers (TMD); (**b**) with spring steel type VE–PTMD; (**c**) with pendulum type VE–PTMD; (**d**) with spring steel type SMA–PTMD; (**e**) with pendulum type SMA–PTMD.

For comparison, the results of free vibration tests are summarized in Table 2. As seen, after installing the TMD, the control time is extended from 26.5 s to 48.8 s, which is 184% of that without control. The response with TMD is worse when compared to the case of without control because the TMD is not optimally designed [88,89]. The addition of the mass, which has a low damping ratio, decreases the overall damping ratio of the entire assembly. Since the TMD is not optimized, the damping ratio stays at a low value. From the Den Hartog analysis [90], this is because the TMD's auxiliary damping is too small, and it is far from the optimal damping. Thus, the TMD cannot dissipate energy effectively and lead to a continual, mutual transmission of energy between the pipe and the TMD. This is the reason for the beating phenomenon and the extension of the control time. In contrast, the control effects of four PTMDs are evident. The control times are from 1.6 s to 2.9 s, which correspond to 6% to 11% of the corresponding time of the piping system without control. This shows that all four PTMDs effectively and efficiently suppress the displacement response of the piping system during the free vibration. With the TMD control, the system damping ratio is reduced from 0.58% to 0.29%; however, the damping ratios are increased significantly with PTMD control (4.0%~10.4%). The damping ratios of the PTMDs are 6.9~17.9 times larger than when there is no control. This shows the effectiveness of when pounding is introduced to increase damping. It should be noted that in addition to rapidly suppressing the vibrations of the piping system, the PTMDs also greatly reduce the amount of strong cycles of vibration. In other words, the system rapidly reaches lower levels of vibration within the first few cycles of vibration, although the time needed to fully suppress vibrations takes longer.

Table 2. The results of free vibration.

Conditions			Time (20 mm to 2 mm)	Damping Ratio
Without Control			26.5 s	0.58%
With TMD Control			48.8 s	0.29%
With PTMD Control	VE	Spring Steel	1.6 s	10.4%
		Pendulum	2.85 s	5.6%
	SMA	Spring Steel	2.5 s	4.9%
		Pendulum	2.9 s	4.0%

5.2. Suppression of Forced Vibration

In forced vibration experiments, a high-power motor with a rotating arm is used to generate a quasi-harmonic excitation. The rotating arm of the motor is connected to the middle of the pipe via a bungee cable, and the bungee cable passes through a pulley to keep the excitation horizontal. The excitations of different frequencies are achieved by adjusting the voltage of the motor and changing the rotational speed of the arm. These kinds of quasi-harmonic excitations have also been used in other pipe tests [38,42,66].

The frequency response curves of the piping system are plotted by recording the steady-state displacement amplitudes over different excitation frequencies of forced vibration. Figure 8 describes the frequency responses of the piping system under the conditions of the piping system without control, with the TMD control, with the spring steel type VE–PTMD control, with the pendulum type VE–PTMD control, with the spring steel type SMA–PTMD control, and with the pendulum type SMA–PTMD control.

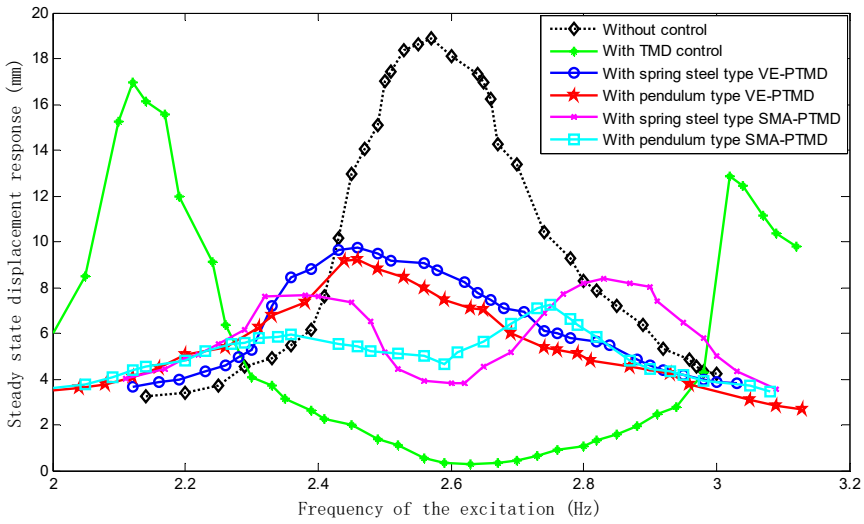

Figure 8. Experimental results of forced vibration.

The resonant frequency of the piping system is measured to be 2.57 Hz, and the maximum displacement of the system at the resonant condition is 18.90 mm. After the addition of TMD, the frequency response curve of the piping system has two peaks, which are on each side of the original resonant frequency, as shown in the green line of Figure 8. The new system's resonant frequencies are 2.12 Hz and 3.02 Hz, and the corresponding magnitudes of vibration are 16.98 mm and 12.86 mm. The blue line and red line are frequency responses of the piping system with the spring steel type VE–PTMD control and with the pendulum type VE–PTMD control. Both curves have only one peak, the resonant frequencies are both 2.46 Hz, and the corresponding magnitudes of vibration are 9.72 mm and 9.24 mm, respectively.

The magenta line and the cyan line represent the frequency responses of the piping system with the spring steel type SMA–PTMD control and with the pendulum type SMA–PTMD control. Similar to the case with the TMD control, both the curves have two magnitude peaks. The peak frequencies of the response with the spring steel type SMA–PTMD are 2.38 Hz and 2.83 Hz, and the corresponding magnitudes are 7.67 mm and 8.39 mm, respectively, as shown by the magenta line in Figure 8. Two peaks of the frequency response with the pendulum type SMA–PTMD control (the cyan line) are 2.36 Hz and 2.75 Hz, and the corresponding magnitudes are 5.93 mm and 7.26 mm. At the resonant frequency of the piping system (2.57 Hz), the control effect of the spring steel type SMA–PTMD (3.91 mm) is slightly better than that of the pendulum type SMA–PTMD (5.0 mm).

In order to understand the effectiveness of SMA–PTMDs at the resonant frequency (2.57 Hz), a lock–release experiment of the PTMD mass is conducted. First, the mass of the PTMDs is locked, and the PTMD and the piping system become one system. At the resonant frequency excitation, the whole system reaches the maximum displacement response. At this point, the constraint of the mass is released and the PTMD starts working. Figure 9 shows the displacement responses of the piping system before and after the mass of the PTMDs is released. After the mass of the PTMDs is released, the mass collides with the pipe, and the displacement of the pipe is rapidly reduced. After this transient process, the displacement of the pipe tends to be stable. In the entire frequency domain, the maximum displacement responses of the piping system with the SMA–PTMDs controls occur at 2.83 Hz (spring steel type) and 2.75 Hz (pendulum type). Figure 10 compares the maximum displacement response without control and with the SMA–PTMDs control. The maximum displacement response with the pendulum type SMA–PTMD control (7.26 mm) is slightly better than that of with the spring steel type SMA–PTMD control (8.39 mm). From a practical perspective, this small difference suggests that in this case, both types of SMA–PTMDs essentially have a similar performance. A minor tuning of either type may cause the performance to become even closer. This close difference was also observed in the prior study with VE–PTMDs [45], suggesting that these two designs have a nearly equal performance in

vibration suppression, and the user is free to choose a design that may better suit their engineering requirements (e.g., available materials).

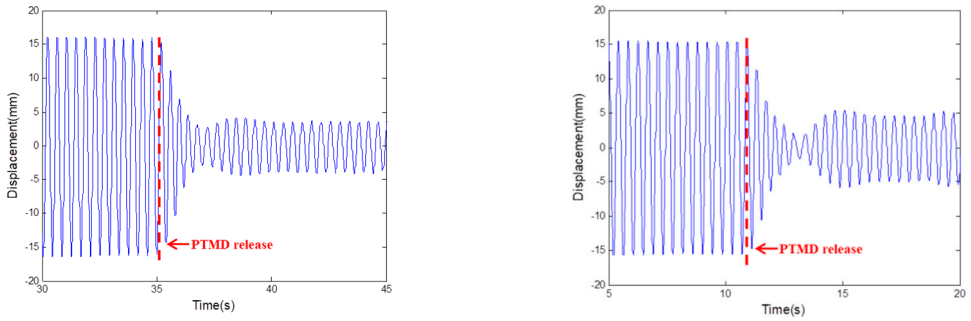

Figure 9. Experimental results of forced vibration when the mass of the SMA–PTMD is released mid-vibration: (**a**) Spring steel type; (**b**) pendulum type.

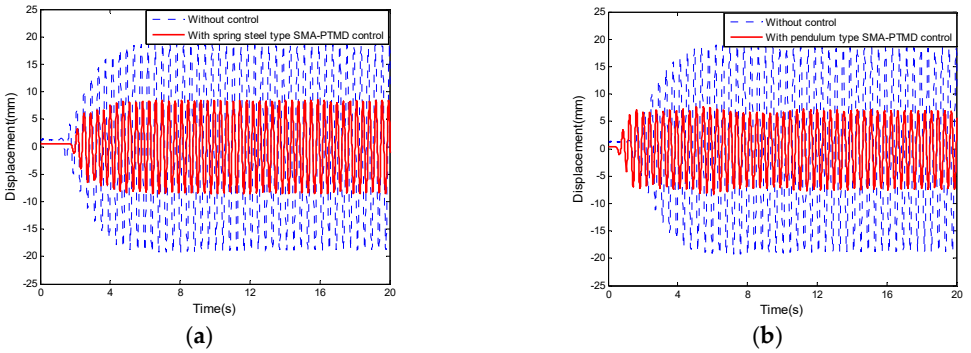

Figure 10. Comparison of resonant vibration with SMA–PTMDs: (**a**) Spring steel type; (**b**) pendulum type.

For comparison, the results are summarized in Table 3. With the TMD control, 97% of displacement is reduced at the resonant frequency (2.57 Hz). However, the reduction comes at the cost of the formation of two new peak regions surrounding the original natural frequency. All four PTMDs, especially the SMA–PTMDs, considerably reduce the displacement responses across the entire frequency domain. From small to large, the amount of vibration reduction can be ordered as: 49% (spring steel type VE–PTMD), 51% (pendulum type VE–PTMD), 56% (spring steel type SMA–PTMD), and 62% (pendulum type SMA–PTMD). At the resonant frequency (2.57 Hz), the displacements of the piping system are 0.54 mm (TMD), 8.99 mm (spring steel type VE–PTMD), 7.89 mm (pendulum type VE–PTMD), 3.91 mm (spring type SMA–PTMD), and 5.00 mm (pendulum type SMA–PTMD). These experimental results demonstrate that the proposed SMA–PTMDs are more effective than VE–PTMDs given the same configuration (i.e., piping system).

Table 3. The results of forced vibration.

Conditions			Resonant Frequency and Corresponding Maximum Displacement		Displacement Reduction Ratio Across the Entire Frequency Domain	Displacement and Reduction Ratio at Resonant Frequency
Without Control			2.57 Hz	18.90 mm	-	-
With TMD Control			2.12 Hz, 3.02 Hz	16.98 mm, 12.86 mm	10%	0.54 mm/97%
With PTMDs control	VE	Spring Steel	2.46 Hz	9.72 mm	49%	8.99 mm/52%
		Pendulum	2.46 Hz	9.24 mm	51%	7.98 mm/58%
	SMA	Spring Steel	2.38 Hz, 2.83 Hz	7.67 mm, 8.39 mm	56%	3.91 mm/79%
		Pendulum	2.36 Hz, 2.75 Hz	5.93 mm, 7.26 mm	62%	5.00 mm/74%

6. Conclusions

The main novelty of this research is development of the shape memory alloy–pounding tuned mass damper (SMA–PTMD) that uses the SMA material to accelerate energy dissipation in a pounding tuned mass damper. In this study, two different types of PTMDs (spring steel type and pendulum type) are equipped with a shape memory alloy sponge to suppress the vibration of a suspended piping system. The SMA–PTMDs are tested in both free vibration and forced vibration cases. To investigate the influence of energy dissipating material (SMA) on the PTMD device, the SMA–PTMD results are compared with those of a previous study by the authors [45], which consists of a TMD control and a VE–PTMDs control.

In the free vibration experiment, the beating phenomenon is observed in the responses of the pipe with the SMA–PTMDs control. The control times are reduced from 26.5 s (without control) to 2.5 s (spring steel type) and 2.9 s (pendulum type). The damping ratios are increased from 0.58% (without control) to 4.9% (spring steel type) and 4.0% (pendulum type). SMA–PTMDs suppress the vibration of the piping system effectively. Both the shortened time and the increased damping show that SMA–PTMDs suppress the vibration of the pipe effectively and efficiently. In the forced vibration experiment, the frequency responses of the piping system under the control of SMA–PTMDs have one peak on each side of the piping system's resonant frequency which are different compared to the single peak frequency responses under the control of VE–PTMDs. By comparing the damping effects of the same types of SMA–PTMDs and VE–PTMDs, it can be observed that SMA material considerably improves the performance of PTMDs both across the entire frequency domain and especially at the resonant frequency.

The results presented in this paper demonstrate the ability of SMA–PTMDs to suppress the vibration of a suspended piping system effectively and efficiently for both free vibration and forced vibration. The numerical model of SMA as a pounding energy dissipating material has not been studied in this paper and will be the subject of future work. Additionally, the nonlinearity of SMA in collision also requires more detailed research.

Author Contributions: All authors discussed and agreed upon the idea and made scientific contributions. J.T., P.Z., and J.J. designed the experiments. J.T. and M.L. performed the experiments and analyzed the data. Q.F. and J.T. wrote the paper. Q.F. and S.C.M.H. revised the paper.

Funding: This work is partially supported by the Scientific Research Fund of the Institute of Seismology and the Institute of Crustal Dynamics, China Earthquake Administration (Grant number IS201616250) and the National Natural Science Foundation of China (Grant number 51808092). The authors would also like to thank the support from the China Scholarship Council.

Conflicts of Interest: The authors declare no conflict of interest.

References

1. Hall, J.F.; Holmes, W.T.; Somers, P. *Northridge Earthquake*; Preliminary reconnaissance report; EERI: Oakland, CA, USA, 1994.
2. Gates, W.E.; McGavin, G. Lessons learned from the 1994 Northridge earthquake on the vulnerability of nonstructural systems. In Proceedings of the Seminar on Seismic Design, Retrofit, and Performance of Nonstructural Components, San Francisco, CA, USA, 22–23 January 1998.
3. Whittaker, A.S.; Soong, T.T. An overview of nonstructural components research at three US Earthquake Engineering Research Centers. In Proceedings of the ATC Seminar on Seismic Design, Performance, and Retrofit of Nonstructural Components in Critical Facilities, Newport Beach, CA, USA, 23–24 October 2003.
4. Taghavi, S.; Miranda, E. *Response Assessment of Nonstructural Building Elements*; Pacific Earthquake Engineering Research Center: Berkeley, CA, USA, 2003.
5. Chock, G. *Preliminary Observations on the Hawaii Earthquakes of October 15, 2006*; EERI special earthquake report; EERI: Oakland, CA, USA, 2006.
6. Miranda, E.; Mosqueda, G.; Retamales, R.; Pekcan, G. Performance of nonstructural components during the 27 February 2010 Chile earthquake. *Earthq. Spectra* **2012**, *28* (Suppl. 1), S453–S471. [CrossRef]

7. Ayres, J.M.; Phillips, R.J. Water damage in hospitals resulting from the Northridge earthquake. *Ashrae Trans.* **1998**, *104*, 1286.
8. Goltz, J. *The Northridge, California Earthquake of January 17, 1994*; General reconnaissance report; National Center for Earthquake Engineering Research: Buffalo, NY, USA, 1994.
9. Fleming, R.P. *Analysis of Fire Sprinkler Systems Performance in the Northridge Earthquake*; (No. Grant/Contract Reports (NISTGCR)-98-736); National Institute of Standards and Technology: Gaithersburg, MD, USA, 1998.
10. Hardy, G.S.; Smith, P.D.; Tang, Y.K. Piping seismic adequacy criteria recommendations based on performance during earthquakes. *Nucl. Eng. Des.* **1988**, *107*, 155–160. [CrossRef]
11. Zaghi, A.E.; Maragakis, E.M.; Itani, A.; Goodwin, E. Experimental and analytical studies of hospital piping assemblies subjected to seismic loading. *Earthq. Spectra* **2012**, *28*, 367–384. [CrossRef]
12. Tian, Y.; Filiatrault, A.; Mosqueda, G. Seismic response of pressurized fire sprinkler piping systems II: Numerical study. *J. Earthq. Eng.* **2015**, *19*, 674–699. [CrossRef]
13. Norris, M.A.; Ptak, K.R.; Zamora, B.A.; Hart, J.D. Implementation of tuned vibration absorbers for above ground pipeline vibration control. In Proceedings of the 2000 3rd International Pipeline Conference, Calgary, AB, Canada, 1–5 October 2000; p. V001T02A005.
14. Kumar, P.; Jangid, R.S.; Reddy, G.R. Comparative performance of passive devices for piping system under seismic excitation. *Nucl. Eng. Des.* **2016**, *298*, 121–134. [CrossRef]
15. Namita, Y.; Shigeta, M.; Yoshinaga, T.; Gotoh, N.; Kawahata, J. The application of elastoplastic support devices for a piping system: Device test and vibration test of piping system and simulation analysis. *JSME Int. J. Ser. 3 Vib. Control Eng. Eng. Ind.* **1991**, *34*, 42–48. [CrossRef]
16. Nims, D. Large-Scale Experimental Studies of Two Alternate Support Systems for the Seismic Restraint of Piping. Ph.D. Thesis, University of California at Berkeley, Berkeley, CA, USA, 1991.
17. Suzuki, K.; Watanabe, T.; Mitsumori, T.; Shimizu, N.; Kobayashi, H.; Ogawa, N. Experimental Study on Seismic Responses of Piping Systems with Friction—Part 1: Large-Scale Shaking Table Vibration Test. *J. Press. Vessel Technol.* **1995**, *117*, 245–249. [CrossRef]
18. Bakre, S.V.; Jangid, R.S.; Reddy, G.R. Response of piping system on friction support to bi-directional excitation. *Nucl. Eng. Des.* **2007**, *237*, 124–136. [CrossRef]
19. Suarez, E.; Roldán, A.; Gallego, A.; Benavent-Climent, A. Entropy analysis for damage quantification of hysteretic dampers used as seismic protection of buildings. *Appl. Sci.* **2017**, *7*, 628. [CrossRef]
20. Kang, J.D.; Mori, Y. Evaluation of a Simplified Method to Estimate the Peak Inter-Story Drift Ratio of Steel Frames with Hysteretic Dampers. *Appl. Sci.* **2017**, *7*, 449. [CrossRef]
21. Fu, W.; Zhang, C.; Sun, L.; Askari, M.; Samali, B.; Chung, K.L.; Sharafi, P. Experimental investigation of a base isolation system incorporating MR dampers with the high-order single step control algorithm. *Appl. Sci.* **2017**, *7*, 344. [CrossRef]
22. Gastaldi, C.; Fantetti, A.; Berruti, T. Forced response prediction of turbine blades with flexible dampers: The impact of engineering modelling choices. *Appl. Sci.* **2018**, *8*, 34. [CrossRef]
23. Huo, L.; Song, G.; Nagarajaiah, S.; Li, H. Semi-active vibration suppression of a space truss structure using a fault tolerant controller. *J. Vib. Control* **2012**, *18*, 1436–1453. [CrossRef]
24. Demetriou, D.; Nikitas, N.; Tsavdaridis, K.D. Semi active tuned mass dampers of buildings: A simple control option. *Am. J. Eng. Appl. Sci.* **2015**, *8*, 620–632. [CrossRef]
25. Li, L.; Song, G.; Ou, J. A genetic algorithm-based two-phase design for optimal placement of semi-active dampers for nonlinear benchmark structure. *J. Vib. Control* **2010**, *16*, 1379–1392. [CrossRef]
26. Kim, B.; Yoon, J.Y. Enhanced Adaptive Filtering Algorithm Based on Sliding Mode Control for Active Vibration Rejection of Smart Beam Structures. *Appl. Sci.* **2017**, *7*, 750. [CrossRef]
27. Lin, C.Y.; Jheng, H.W. Active vibration suppression of a motor-driven piezoelectric smart structure using adaptive fuzzy sliding mode control and repetitive control. *Appl. Sci.* **2017**, *7*, 240. [CrossRef]
28. Gu, H.; Song, G. Active vibration suppression of a flexible beam with piezoceramic patches using robust model reference control. *Smart Mater. Struct.* **2007**, *16*, 1453. [CrossRef]
29. Kim, H.; Adeli, H. Hybrid control of smart structures using a novel wavelet-based algorithm. *Comput. Aided Civ. Infrastruct. Eng.* **2005**, *20*, 7–22. [CrossRef]
30. Ozbulut, O.E.; Hurlebaus, S. Application of an SMA-based hybrid control device to 20-story nonlinear benchmark building. *Earthq. Eng. Struct. Dyn.* **2012**, *41*, 1831–1843. [CrossRef]

31. Demetriou, D.; Nikitas, N. A novel hybrid semi-active mass damper configuration for structural applications. *Appl. Sci.* **2016**, *6*, 397. [CrossRef]
32. Palacios-Quiñonero, F.; Rubió-Massegú, J.; Rossell, J.M.; Karimi, H.R. Integrated design of hybrid interstory-interbuilding multi-actuation schemes for vibration control of adjacent buildings under seismic excitations. *Appl. Sci.* **2017**, *7*, 323. [CrossRef]
33. Lu, Z.; Chen, X.; Zhang, D.; Dai, K. Experimental and analytical study on the performance of particle tuned mass dampers under seismic excitation. *Earthq. Eng. Struct. Dyn.* **2017**, *46*, 697–714. [CrossRef]
34. Chen, J.; Lu, G.; Li, Y.; Wang, T.; Wang, W.; Song, G. Experimental study on robustness of an eddy current-tuned mass damper. *Appl. Sci.* **2017**, *7*, 895. [CrossRef]
35. Kaloop, M.R.; Hu, J.W.; Bigdeli, Y. Identification of the response of a controlled building structure subjected to seismic load by using nonlinear system models. *Appl. Sci.* **2016**, *6*, 301. [CrossRef]
36. Song, G.; Li, L.; Singla, M.; Mo, Y.L. Pounding Tune Mass Damper with Viscoelastic Material. U.S. Patent 9 2016,500,247, 22 November 2016.
37. Wang, W.; Hua, X.; Wang, X.; Chen, Z.; Song, G. Numerical modeling and experimental study on a novel pounding tuned mass damper. *J. Vib. Control* **2018**, *24*, 4023–4036. [CrossRef]
38. Jiang, J.; Zhang, P.; Patil, D.; Li, H.N.; Song, G. Experimental studies on the effectiveness and robustness of a pounding tuned mass damper for vibration suppression of a submerged cylindrical pipe. *Struct. Control Health Monit.* **2017**, *24*, e2027. [CrossRef]
39. Xue, Q.; Zhang, J.; He, J.; Zhang, C. Control performance and robustness of pounding tuned mass damper for vibration reduction in SDOF structure. *Shock Vib.* **2016**, *2016*, 8021690. [CrossRef]
40. Zhang, P.; Song, G.; Li, H.N.; Lin, Y.X. Seismic control of power transmission tower using pounding TMD. *J. Eng. Mech.* **2012**, *139*, 1395–1406. [CrossRef]
41. Lin, W.; Wang, Q.; Li, J.; Chen, S.; Qi, A. Shaking table test of pounding tuned mass damper (PTMD) on a frame structure under earthquake excitation. *Comput. Concr.* **2017**, *20*, 545–553.
42. Li, H.-N.; Zhang, P.; Song, G.; Patil, D.; Mo, Y. Robustness study of the pounding tuned mass damper for vibration control of subsea jumpers. *Smart Mater. Struct.* **2015**, *24*, 095001. [CrossRef]
43. Song, G.; Zhang, P.; Li, L.Y.; Singla, M.; Patil, D.; Li, H.N.; Mo, Y.L. Vibration control of a pipeline structure using pounding tuned mass damper. *J. Eng. Mech.* **2016**, *142*, 04016031. [CrossRef]
44. Lin, W.; Song, G.; Chen, S. PTMD control on a benchmark TV tower under earthquake and wind load excitations. *Appl. Sci.* **2017**, *7*, 425. [CrossRef]
45. Tan, J.; Ho, M.; Chun, S.; Zhang, P.; Jiang, J. Experimental Study on Vibration Control of Suspended Piping System by Single-Sided Pounding Tuned Mass Damper. *Appl. Sci.* **2019**, *9*, 285. [CrossRef]
46. Ren, W.; Li, H.; Song, G. Phenomenological modeling of the cyclic behavior of superelastic shape memory alloys. *Smart Mater. Struct.* **2007**, *16*, 1083. [CrossRef]
47. Sun, M.; Chang, M.; Wang, Z.; Li, H.; Sun, X. Experimental and Simulation Study of Low-Velocity Impact on Glass Fiber Composite Laminates with Reinforcing Shape Memory Alloys at Different Layer Positions. *Appl. Sci.* **2018**, *8*, 2405. [CrossRef]
48. Hong, K.; Lee, S.; Han, S.; Yeon, Y. Evaluation of Fe-Based Shape Memory Alloy (Fe-SMA) as Strengthening Material for Reinforced Concrete Structures. *Appl. Sci.* **2018**, *8*, 730. [CrossRef]
49. Seo, J.; Kim, Y.C.; Hu, J.W. Pilot study for investigating the cyclic behavior of slit damper systems with recentering shape memory alloy (SMA) bending bars used for seismic restrainers. *Appl. Sci.* **2015**, *5*, 187–208. [CrossRef]
50. Qian, H.; Li, H.; Song, G. Experimental investigations of building structure with a superelastic shape memory alloy friction damper subject to seismic loads. *Smart Mater. Struct.* **2016**, *25*, 125026. [CrossRef]
51. Xu, M.B.; Song, G. Adaptive control of vibration wave propagation in cylindrical shells using SMA wall joint. *J. Sound Vib.* **2004**, *278*, 307–326. [CrossRef]
52. Rustighi, E.; Brennan, M.J.; Mace, B.R. Real-time control of a shape memory alloy adaptive tuned vibration absorber. *Smart Mater. Struct.* **2005**, *14*, 1184–1195. [CrossRef]
53. Rustighi, E.; Brennan, M.J.; Mace, B.R. A shape memory alloy adaptive tuned vibration absorber: Design and implementation. *Smart Mater. Struct.* **2004**, *14*, 19–28. [CrossRef]
54. Santos, F.A.D.; Nunes, J. Toward an adaptive vibration absorber using shape-memory alloys, for civil engineering applications. *J. Intell. Mater. Syst. Struct.* **2018**, *29*, 729–740. [CrossRef]

55. Williams, K.A.; Chiu, G.T.C.; Bernhard, R.J. Nonlinear control of a shape memory alloy adaptive tuned vibration absorber. *J. Sound Vib.* **2005**, *288*, 1131–1155. [CrossRef]
56. Williams, K.; Chiu, G.; Bernhard, R. Adaptive-passive absorbers using shape-memory alloys. *J. Sound Vib.* **2002**, *249*, 835–848. [CrossRef]
57. Berardengo, M.; Cigada, A.; Guanziroli, F.; Manzoni, S. Modelling and control of an adaptive tuned mass damper based on shape memory alloys and eddy currents. *J. Sound Vib.* **2015**, *349*, 18–38. [CrossRef]
58. Savi, M.A.; De Paula, A.S.; Lagoudas, D.C. Numerical investigation of an adaptive vibration absorber using shape memory alloys. *J. Intell. Mater. Syst. Struct.* **2011**, *22*, 67–80. [CrossRef]
59. Aguiar, R.A.; Savi, M.A.; Pacheco, P.M. Experimental investigation of vibration reduction using shape memory alloys. *J. Intell. Mater. Syst. Struct.* **2013**, *24*, 247–261. [CrossRef]
60. Berardengo, M.; Della Porta, G.E.; Manzoni, S.; Vanali, M. A multi-modal adaptive tuned mass damper based on shape memory alloys. *J. Intell. Mater. Syst. Struct.* **2019**, *30*, 536–555. [CrossRef]
61. Senthilkumar, P.; Umapathy, M. Use of load generated by a shape memory alloy for its position control with a neural network estimator. *J. Vib. Control* **2014**, *20*, 1707–1717. [CrossRef]
62. Wang, W.; Wang, X.; Hua, X.; Song, G.; Chen, Z. Vibration control of vortex-induced vibrations of a bridge deck by a single-side pounding tuned mass damper. *Eng. Struct.* **2018**, *173*, 61–75. [CrossRef]
63. Feng, Q.; Fan, L.; Huo, L.; Song, G. Vibration Reduction of an Existing Glass Window through a Viscoelastic Material-Based Retrofit. *Appl. Sci.* **2018**, *8*, 1061. [CrossRef]
64. Wang, W.; Hua, X.; Wang, X.; Chen, Z.; Song, G. Advanced Impact Force Model for Low-Speed Pounding between Viscoelastic Materials and Steel. *J. Eng. Mech.* **2017**, *143*, 04017139. [CrossRef]
65. Bonfitto, A.; Tonoli, A.; Amati, N. Viscoelastic Dampers for Rotors: Modeling and Validation at Component and System Level. *Appl. Sci.* **2017**, *7*, 1181. [CrossRef]
66. Zhang, P.; Li, L.; Patil, D.; Singla, M.; Li, H.N.; Mo, Y.L.; Song, G. Parametric study of pounding tuned mass damper for subsea jumpers. *Smart Mater. Struct.* **2015**, *25*, 015028. [CrossRef]
67. Wang, W.; Hua, X.; Wang, X.; Chen, Z.; Song, G. Optimum design of a novel pounding tuned mass damper under harmonic excitation. *Smart Mater. Struct.* **2017**, *26*, 055024. [CrossRef]
68. Song, G.; Ma, N.; Li, H.N. Applications of shape memory alloys in civil structures. *Eng. Struct.* **2006**, *28*, 1266–1274. [CrossRef]
69. Sawaguchi, T.; Maruyama, T.; Otsuka, H.; Kushibe, A.; Inoue, Y.; Tsuzaki, K. Design concept and applications of Fe–Mn–Si-based alloys—From shape-memory to seismic response control. *Mater. Trans.* **2016**, *57*, 283–293. [CrossRef]
70. Jani, J.M.; Leary, M.; Subic, A.; Gibson, M.A. A review of shape memory alloy research, applications and opportunities. *Mater. Des. (1980–2015)* **2014**, *56*, 1078–1113. [CrossRef]
71. Menna, C.; Auricchio, F.; Asprone, D. Applications of shape memory alloys in structural engineering. In *Shape Memory Alloy Engineering*; Heinemann: Butterworth, Malaysia, 2015; pp. 369–403.
72. Ren 2015, W.; Li, H.; Song, G. A one-dimensional strain-rate-dependent constitutive model for superelastic shape memory alloys. *Smart Mater. Struct.* **2007**, *16*, 191. [CrossRef]
73. Saadat, S.; Salichs, J.; Noori, M.; Hou, Z.; Davoodi, H.; Bar-On, I.; Suzuki, Y.; Masuda, A. An overview of vibration and seismic applications of NiTi shape memory alloy. *Smart Mater. Struct.* **2002**, *11*, 218. [CrossRef]
74. Li, H.N.; Qian, H.; Song, G.B.; Gao, D.W. Type of shape memory alloy damper: Design, experiment and numerical simulation. *J. Vib. Eng.* **2008**, *21*, 179–184.
75. Li, H.; Liu, Z.Q.; Ou, J.P. Experimental study of a simple reinforced concrete beam temporarily strengthened by SMA wires followed by permanent strengthening with CFRP plates. *Eng. Struct.* **2008**, *30*, 716–723. [CrossRef]
76. Dolce, M.; Cardone, D.; Marnetto, R. Implementation and testing of passive control devices based on shape memory alloys. *Earthq. Eng. Struct. Dyn.* **2000**, *29*, 945–968. [CrossRef]
77. Zhou, P.; Liu, M.; Li, H.; Song, G. Experimental investigations on seismic control of cable-stayed bridges using shape memory alloy self-centering dampers. *Struct. Control Health Monit.* **2018**, *25*, e2180. [CrossRef]
78. Li, H.; Liu, M.; Ou, J. Vibration mitigation of a stay cable with one shape memory alloy damper. *Struct. Control Health Monit.* **2004**, *11*, 21–36. [CrossRef]
79. Wilde, K.; Gardoni, P.; Fujino, Y. Base isolation system with shape memory alloy device for elevated highway bridges. *Eng. Struct.* **2000**, *22*, 222–229. [CrossRef]

80. Dolce, M.; Cardone, D.; Marnetto, R. SMA recentering devices for seismic isolation of civil structures. In *Smart Structures and Materials 2001: Smart Systems for Bridges, Structures, and Highways*; International Society for Optics and Photonics: Newport Beach, CA, USA, 2001; Volume 4330, pp. 238–250.
81. Khan, M.M.; Lagoudas, D.C. Modeling of shape memory alloy pseudoelastic spring elements using Preisach model for passive vibration isolation. In *Smart Structures and Materials 2002: Modeling, Signal Processing, and Control*; International Society for Optics and Photonics: San Diego, CA, USA, 2002; Volume 4693, pp. 336–348.
82. Mayes, J.; Lagoudas, D.; Henderson, B. An experimental investigation of shape memory alloy springs for passive vibration isolation. In Proceedings of the AIAA Space 2001 Conference and Exposition, Albuquerque, NM, USA, 28–30 August 2001; p. 4569.
83. Corbi, O. Shape memory alloys and their application in structural oscillations attenuation. *Simul. Model. Pract. Theory* **2003**, *11*, 387–402. [CrossRef]
84. Miller, D.J.; Fahnestock, L.A.; Eatherton, M.R. Development and experimental validation of a nickel–titanium shape memory alloy self-centering buckling-restrained brace. *Eng. Struct.* **2012**, *40*, 288–298. [CrossRef]
85. Huang, B.; Zhang, H.; Wang, H.; Song, G. Passive base isolation with superelastic nitinol SMA helical springs. *Smart Mater. Struct.* **2014**, *23*, 065009. [CrossRef]
86. Asgarian, B.; Moradi, S. Seismic response of steel braced frames with shape memory alloy braces. *J. Constr. Steel Res.* **2011**, *67*, 65–74. [CrossRef]
87. DDS Simulia, ABAQUS Unified FEA Software. Available online: www.3ds.com (accessed on 1 March 2019).
88. Tributsch, A.; Adam, C. Evaluation and analytical approximation of tuned mass damper performance in an earthquake environment. *Smart Struct. Syst.* **2012**, *10*, 155–179. [CrossRef]
89. Anajafi, H.; Medina, R.A. Comparison of the seismic performance of a partial mass isolation technique with conventional TMD and base-isolation systems under broad-band and narrow-band excitations. *Eng. Struct.* **2018**, *158*, 110–123. [CrossRef]
90. Den Hartog, J.P. *Mechanical Vibrations*; Courier Corporation: North Chelmsford, MA, USA, 1985.